High-performance CO_2 sorbents from algae

Marta Sevilla,[a*] Camillo Falco,[b,c] Maria-Magdalena Titirici,[c] Antonio B. Fuertes[a]

Abstract

Highly porous N-doped carbon materials with apparent surface areas in the 1300 - 2400 m^2 g^{-1} range and pore volumes up to 1.2 cm^3 g^{-1} have been synthesized from hydrothermal carbons obtained from mixtures of algae and glucose. The porosity of these materials is made up of uniform micropores, most of them having sizes < 1 nm. Moreover, they have N contents in the 1.1 - 4.7 wt% range, this heteroatom being mainly as pyridone-type structures. These microporous carbons present unprecedented large CO_2 capture capacities, up to 7.4 mmol g^{-1} (1 bar, 0 ºC). The importance of the pore size on the CO_2 capture capacity of microporous carbon materials is clearly demonstrated. Indeed, a good correlation between the CO_2 capture capacity at sub-atmospheric pressure and the volume of narrow micropores is observed. The results suggest that pyridinic-N, pyridonic/pyrrolic-N and quaternary-N do not contribute significantly to the CO_2 adsorption capacity, owing probably to their low basicity in comparison with amines. These findings point out a key for the design of high-performance CO_2 capture sorbents.

1. Introduction

The growing environmental concerns for global warming and climate change are reflected in the increasing number of works related to the development of more-efficient and improved processes for CO_2 capture and storage. Capturing CO_2 is by far the most energy-expensive part of carbon capture and storage technologies. In this regard, physisorption of CO_2 in porous solids using pressure, temperature or vacuum swing adsorption processes (PSA, TSA or VSA respectively) can significantly decrease the cost, as well as the environmental impact associated to the current used technologies involving amines. A CO_2 sorbent should satisfy the following requirements: (i) large CO_2 uptake, (ii) high sorption rate, (iii) good selectivity between CO_2 and other competing gases in the stream (i.e. N_2), (iv) easy regeneration and (v) low-cost and high availability. So far, numerous porous solids have been investigated, such as zeolites, metal-organic frameworks (MOFs), polymers, porous carbons including templated carbons, activated carbons and carbide-derived carbons (CDCs), or organic-inorganic hybrid materials.[1-6] Among them, porous carbons stand out in terms of cost, stability, availability, large surface area, easy-to-design pore structure and low energy requirements for regeneration. More specifically, activated carbons continue to be the primary choice for many adsorption-based processes due to their cost-availability and microstructure. In this regard, research on novel activation procedures which allow better controlled microstructure and PSD is crucial for further development of many adsorption-based systems, such as hydrogen storage, supercapacitors or CO_2 capture. However, not only the activation conditions influence the microstructure of the final material, but also the precursor used. For a large-scale sustainable production, naturally grown materials should be used as precursor. In this respect, biomass is highly attractive. More specifically, microalgae stand out for very high photosynthesis

efficiency and are considered a fast growing biomass, commonly doubling their mass within a 24 h growth window.[7-10] which would ensure quick availability of this precursor. An additional advantage of microalgae is that some species are rich in proteins and therefore have relatively high nitrogen contents, which may allow the synthesis of N-doped materials. The synthesis of this kind of materials is receiving increasing attention as the presence of nitrogen confers the carbon material improved thermal/oxidation stability and higher electrical conductivity.[11,12] Furthermore, nitrogen-containing functionalities are responsible for an increase in the surface polarity of carbon and for basicity,[13] which could enhance the interaction between carbon and acid molecules, such as H_2S, SO_2 or CO_2. In the present work, we will prove the efficient transformation of a microalgae-derived N-doped hydrothermal carbon into highly microporous N-doped carbon materials. In addition, we analyzed their CO_2 capture capacity, and found that those microporous carbons presented unprecedented large CO_2 uptakes for carbon materials, up to 7.4 mmol g^{-1} at 0 ºC and 1 bar. Their capture capacity has been correlated with their chemical and textural characteristics, showing that the volume of narrow micropores is the parameter governing the adsorption of CO_2 at sub-atmospheric conditions.

2. Experimental Section

2.1. Preparation of activated carbons

N-doped hydrothermal carbon materials (HTC carbon) were obtained by hydrothermal co-carbonization of microalgae (*Spirulina Platensis*) and glucose, with a mass ratio microalgae/glucose = 1.5, at a temperature of 200ºC for 24 h. Afterwards, the hydrothermal carbons were chemically activated in a vertical furnace using potassium hydroxide (Sigma-Aldrich) at temperatures in the range 650 - 750 ºC and KOH/HTC

carbon mass ratio of 1, 2 or 4. The samples were denoted as AG-x-T, where x is the mass ratios KOH/HTC carbon and T the activation temperature.

2.2 Sample characterization

Elemental Analysis (C, H, N, S and O) was carried out on a LECO CHN-932 microanalyzer. X-ray photoelectron spectroscopy (XPS) was carried out by means of a Thermo Scientific K-Alpha ESCA instrument using monochromatic Al-Kα radiation (hν = 1486.6 eV). Binding energies for the high-resolution spectra were calibrated by setting C 1s at 285.0 eV. SEM images were SEM images were acquired on a LEO 1550/LEO GmbH Oberkochen equipped with an Everhard Thornley secondary electron and in-lens detectors. Nitrogen sorption isotherms of the carbon samples were measured at −196 °C using a Micromeritics ASAP 2020 sorptometer. The apparent surface area was calculated using the BET method; for the selection of the appropriate relative pressure range, the ISO 9277:2010 was followed.[14] The total pore volume was determined from the amount of nitrogen adsorbed at a relative pressure (P/P$_0$) of 0.99, whereas the micropore volume, V$_0$, and narrow micropore volume, V$_n$, where determined by applying the Dubinin–Radushkevich (DR) equation to the nitrogen and carbon dioxide isotherms respectively. The average pore width, L$_0$, was calculated by application of the equation proposed by Stoeckli and Ballerini.[15] The pore size distribution (PSD) was determined via a Quench Solid State Functional Theory (QSDFT) method (implemented into Quantachrome's data software), using nitrogen adsorption data, and assuming a slit-shaped pore model. This method supposes an improvement over the non-local density functional method (NLDFT), allowing one to account explicitly for the effects of surface heterogeneity, typical in activated carbons.[16,17] The false gaps at around 1 and 2 nm, which are typical artifacts of the

standard NLDFT model that treats the pore walls as homogeneous graphite-like plane surfaces, disappear in the QSDFT PSD.

CO₂ Adsorption Measurements. The adsorption of CO_2 was measured using a Nova 200e (Quantachrome) static volumetric analyzer. Prior to the adsorption analysis, the sample was degassed at 200 °C for several hours. The CO_2 adsorption experiments were performed at three temperatures: 0 °C, 25 °C, and 50 °C. The adsorption kinetics of the CO_2 and N_2, and adsorption-desorption cycles were measured in a thermogravimetric analyser (C. I. Electronics). Both sets of experiments were performed at 25 ° C and the temperature was controlled by means of a circulating bath (Haake K15). For the kinetics analysis, the sample ($\approx$ 50 mg) was degassed under a He stream at 200 °C for 1 h. The gas was then switched from He to CO_2 or N_2 (100 mL/ min) and the weight variation with time was recorded. In the case of the adsorption-desorption cycles, the sample ($\approx$ 50 mg) was degassed under a stream of He at a temperature of 200 °C before the cyclic experiments. During the adsorption, the carbon sample was exposed to a stream of pure CO_2 (100 mL/min). Once the sample was saturated, the gas was switched back from CO_2 to He (100 mL/min) and the carbon dioxide was desorbed. This adsorption–desorption cycle was repeated several times.

3. Results and discussion

In a previous work, we showed that hydrothermal co-carbonization of a protein rich microalgae, i.e. *Spirulina Platensis*, with glucose at T = 200 ºC for 24 h yields a N-doped hydrothermal carbon with a N content of 7.5 wt % and lacking framework confined porosity (S_{BET} ~ 6 m² g⁻¹).[18] As shown in Figure S1a in Supporting Information, this material is composed mostly of spheroidal particles with rough surface. After the chemical activation step, a complete change in the morphology of the

particles takes place, as can be seen in Figure S1b. Now the material is composed of particles of irregular morphology and sharp edges with a surface apparently smooth. However, higher magnification SEM micrographs reveal a high degree of surface roughness, present as well inside the particles (see Figure S1c), which highlights the presence of porosity. This complete rearrangement of the particles morphology suggests melting down of the precursor during the activation process. This behavior has been previously observed for hydrothermal carbons obtained from a variety of saccharides or biomass, like glucose, starch or sawdust.[19] However, when more carbonized materials, i.e. materials with a more rigid structure, such as templated carbons[20] or carbide-derived carbons[21] are used as precursors, the structure of the initial material is partially preserved. This allows the creation of a large amount of porosity. Thus, highly porous materials with apparent surface areas in the ~1300 – 2400 m^2 g^{-1} range and pore volumes up to ~ 1.2 cm^3 g^{-1} are obtained (see Table 1). They all exhibit type I isotherms, with a more or less pronounced knee depending on the activation conditions (Figure S2 in SI). As shown by their QSDFT pore size distributions depicted in Figure 1, they are exclusively microporous (pores < 2 nm), except for the highly activated samples (650-700°C and KOH/HTC carbon = 4), which also exhibit a small amount of mesopores up to 3 nm. Furthermore, the main pore size system is below 1 nm in all the samples, which is a very desirable feature for CO_2 capture, as CO_2 adsorption is strongly favored in such micropores.[1,22] Comparison of the PSD of samples activated at increasing temperature for the same KOH/HTC carbon ratio reveals an increase of the average pore size, as well as a broadening of the PSD. The same effect on the PSD is caused by the increase of the KOH/HTC carbon ratio at a fixed activation temperature. This enlargement of the porosity is accompanied by an increase of both the apparent surface area and total pore volume (see Figure S3 in Supporting Information). It must be

mentioned that direct activation with KOH of the algae leads to its complete burn-off. Therefore, hydrothermal carbonization is a key step to the successful conversion of algae into a product of high-added value, i.e. an activated carbon with excellent CO_2 capture capacity, as will be here proved.

The results of the elemental analysis gathered in Table 1 show that the KOH activation leads to the partial loss of nitrogen contained in the precursor, from 7.5 wt% in the hydrothermal carbon to 1.1 - 4.7 wt% in the activated carbons. The preferential removal of N during the activation process has been already reported by other authors for other nitrogen-containing precursors.[23-25] The nature of the nitrogen moieties on the carbon surface was analyzed by XPS, results shown in Figure 2a for a representative sample, i.e. AG-2-650. Three main contributions are visible in the high-resolution N 1s: i) pyridinic-N at 398.8 eV, ii) pyrrolic-/pyridonic-N at 400.1 eV and iii) quaternary-N at 401.5 eV. Although pyrrolic-N and pyridonic-N are indistinguishable by XPS, taking into account the conditions of the activation process, e.g. oxidative environment and high temperatures (> 600ºC), the peak at 400.1 eV is most likely attributed to pyridone-type structures.[26] We would like to stress the fact that in all the prepared porous carbons, the pyridone-type structures are the main type of N-functionalities. These N-moieties confer Lewis basicity to the materials, which might be relevant for the capture of acidic gases such as CO_2.

These microporous carbons were investigated as CO_2 sorbents at sub-atmospheric conditions (up to 1 bar), typical for post-combustion capture. The results are summarized in Table 2. All the materials exhibit excellent CO_2 capture capacities, higher than 5.9 mmol CO_2 g^{-1} (260 mg CO_2 g^{-1} or 26 %) at 0ºC and 1 bar. Especially remarkable are the values obtained for AG-2-650 and AG-2-700, i.e. 7.0 and 7.4 mmol CO_2 g^{-1} respectively, which are among the highest ever reported for porous carbon

materials (see Table 3). Only Presser et al. reported a value of 7.1 mmol CO_2 g^{-1} at 0 ºC and 1 bar for a carbide-derived carbon (CDC),[1] and Wahby et al. a value of 8.6 mmol CO_2 g^{-1} (0 ºC) for a petroleum pitch-derived activated carbon.[27] Even at 50ºC, the CO_2 capture capacity of such sustainable carbon materials is significant, in the 2.2 to 2.8 mmol CO_2 g^{-1} range. As expected for an exothermic process, the amount of CO_2 adsorbed decreases with the increase in adsorption temperature. To determine the strength of the interaction between CO_2 molecules and the porous sorbents, the isosteric heat of adsorption was calculated by applying the Clausius–Clapeyron equation to the adsorption isotherms. The values found for these materials are in the 22 - 30 kJ/mol range, typical for a physisorption process and similar to other activated carbons.[22,28] Those values are lower than for amine-functionalized materials, which are in the 40 - 90 kJ/mol range.[29-31] This result suggests that the N functionalities present in these materials do not interact significantly with CO_2 molecules, so that the adsorption of CO_2 will be governed by the textural properties (*vide infra*). It should be mentioned that Simmons et al. showed for MOFs that, under typical swing adsorption processes, which are widely used in industrial processing, an isosteric heat of adsorption between 22 and 28 kJ/mol is optimal for single-component CO_2 streams and between 26 and 31 kJ/mol for a 20 % partial pressure CO_2 flue gas.[32] Taking this into account, these materials would be highly suitable for such CO_2 capture systems. To further probe such statement, the regeneration of the sorbents was studied. To test the regeneration of the carbon sorbents, adsorption (CO_2 at 1 bar)-desorption (under He) cycles were performed at 25 ºC in a TGA system. The results are shown in Figure 3a for the CO_2 sorbent with the highest uptake (AG-2-700). It can be seen that both CO_2 adsorption and desorption processes are very fast, taking place in a span of 6 min. Furthermore, the adsorption-desorption cycles can be repeated several times and no noticeable changes are observed

in the sorption kinetics nor CO_2 uptake. This result is in agreement with the relatively weak interaction between CO_2 and these sorbents.

To probe the selectivity of the sorbents against the major component in flue gas, i.e. N_2 (> 70 %), N_2 isotherms were also measured at 25 °C for two sorbents, AG-2-650 and AG-2-700 (see Figure 3b). In both cases, the amount of N_2 adsorbed is much lower than the amount of CO_2 (0.43 and 0.44 mmol g^{-1} for AG-2-650 and AG-2-700 respectively), which yields a good CO_2/N_2 equilibrium selectivity of around 10 in both cases.

The correlation of the textural and chemical characteristics of these materials with their CO_2 adsorption capacity can provide useful information for the design of high-performance CO_2 capture sorbents. In this respect, we found that no correlation exists between the apparent surface area nor the total pore volume and the CO_2 uptake at 0 °C and 1 bar (likewise for 25 °C) (Figure S4). The same behavior is observed for activated carbons prepared from HTC sawdust, cellulose and starch (see Figure S4),[22] activated templated carbons,[33] microporous organic polymers[4] and carbide-derived carbons.[1] Presser et al. found, however, a linear correlation between the CO_2 uptake at 0 °C and 1 bar and the volume of pores smaller than 0.8 nm determined applying the NLDFT method to the CO_2 adsorption isotherm at 0 °C for CDCs and activated CDCs.[1] The same trend is observed here when the CO_2 uptake at 0 or 25 °C and 1 bar is depicted *vs.* the volume of narrow micropores (< 0.7 - 0.8 nm) determined by applying the Dubinin-Radushkevitch equation to the CO_2 isotherm (V_n (CO_2)), as shown in Figure 4a for 25 °C. Furthermore, the same trend is found for HTC sawdust-, cellulose- and starch-based porous carbons, materials that exhibited also a remarkable performance in CO_2 capture,[22] and for a variety of porous carbon materials, including N-doped carbons (with similar N-moieties to the materials here synthesized), that can be found in the literature (see Figure 4a).[2, 34-38] These findings indicate that the adsorption of CO_2 at sub-

atmospheric conditions by porous materials is governed by the volume of narrow micropores and confirm the theoretical calculations that show that only pores of less than 1 nm can be effective for CO_2 adsorption at atmospheric pressure.[39,40] What is more, independently of the N or O contents of the samples, they all fit the same trend. This suggests a minor contribution of those functionalities to the CO_2 uptake in comparison to the volume of narrow micropores, which is related to the non-polarity and weak polarizability of the CO_2 molecule.[41-43] In this respect, previous excellent performances that have been attributed to the N present in the carbon materials (excluding amine functionalization) would be actually due to their narrow microporosity development. Further evidences of the influence of the pore size in the CO_2 capture capacity is observed when the CO_2 uptake per volume of micropores (V_0 (N_2)) is represented vs. average pore width, L_0 (see Figure 4b). Thus, a clear decrease of the CO_2 uptake per volume of micropores is registered with the enlargement of the average pore width for a variety of porous carbon materials. This behavior is similar to that observed for hydrogen adsorption.[44] Overall, the results here presented indicate that the pore size is the key parameter that should be controlled in the design of porous sorbents for CO_2 capture, trying to maximize the volume of narrow micropores. On the other hand, N-doping should be performed selectively to introduce amines, as less basic functionalities do not interact significantly with CO_2 molecules.

4. Conclusion

In conclusion, we have shown a promising approach for the synthesis of carbon-based sorbents for CO_2 capture. It is based on a green and sustainable approach, i.e. the hydrothermal carbonization of biomass, which enables the transformation of microalgae into a highly microporous N-doped carbon material through a subsequent step of chemical activation. We have shown that the control of the activation conditions

(temperature and amount of KOH) allows the synthesis of exclusively microporous biomass-based materials. These materials possess apparent surface areas in the ~ 1300 – 2400 m^2 g^{-1} range and pore volumes up to ~ 1.2 cm^3 g^{-1}. They additionally exhibit N contents in the 1.1 - 4.7 wt% range, this heteroatom being mainly present as pyridone-type structures. When tested as CO_2 sorbents at sub-atmospheric conditions, they show large CO_2 capture capacities, among the highest for porous materials, up to 7.4 mmol g^{-1} at 0 ºC and 1 bar. This large CO_2 capture capacity is exclusively due to their high volume of narrow micropores and not to the high surface areas or pore volumes, neither to the presence of heteroatoms. This result is a key point for the future design of high-performance CO_2 sorbents. Additionally, those sorbents are easily and completely regenerated, without the energy-penalty associated to the use of amine-based sorbents or systems.

Notes

[a] Instituto Nacional del Carbón (CSIC), P.O. Box 73, 33080 Oviedo, Spain. Fax: +34 985 29 76 62; Tel: +34 985 11 90 90; E-mail: martasev@incar.csic.es (M. Sevilla)
[b] IASS – Institute for Advanced Sustainability Studies, Berliner Strasse 130, 14467, Potsdam (Germany)
[c] Colloid Chemistry, Max-Planck Institute for Colloids and Interfaces, Am Muhlenberg 1, 14476, Potsdam (Germany)

†Electronic Supplementary Information (ESI) available: SEM images of N-doped hydrothermal carbon and N-doped activated carbon, N_2 phyisisorption isotherms of the activated carbons, Evolution of the apparent surface area and pore volume with the increase of the activation temperature for different KOH/HTC carbon weight ratios and correlation between the a) apparent surface area and b) total pore volume and the CO_2 uptake (at 0 ºC and 1 bar) of the porous carbon materials

References

1.   V. Presser, J. McDonough, S. H. Yeon and Y. Gogotsi, *Energy Environ. Sci.,* 2011, **4**, 3059-3066

2.   Y. Xia , R. Mokaya , G. S. Walker and Y. Zhu, *Adv. Energy Mater.,* 2011, **1**, 678-683

3.   D. D'Alessandro , B. Smit and J. Long, *Angew. Chem. Int. Ed.,* 2010, **49**, 6058-6082

4.   R. Dawson , E. Stockel , J. R. Holst , D. J. Adams and A. I. Cooper, *Energy Environ. Sci.,* 2011, **4**, 4239-4245

5.   N. Hedin , L. Chen and A. Laaksonen, *Nanoscale,* 2010, **2**, 1819-1841

6.   S. Choi , J. Drese and C. Jones, *ChemSusChem,* 2009, **2**, 796-854

7.   M. Frac , S. Jezierska-Tys and J. Tys, *Afr. J. Biotechnol.,* 2010, **9**, 9227-9236

8.   Y. Chisti, *Trends Biotechnol.,* 2008, **26**, 126-131

9.   J. Singh and S. Gu, *Renew. Sust. Energ. Rev.,* 2010, **14**, 2596-2610

10.   A. Demirbas and M. Fatih Demirbas, *Energy Conv. Manag.,* 2011, **52**, 163-170

11.   M. Terrones , P. M. Ajayan , F. Banhart , X. Blase , D. L. Carroll , J. C. Charlier, R. Czerw , B. Foley , N. Grobert , R. Kamalakaran , P. Kohler-Redlich , M. Rühle , T. Seeger and H. Terrones, *Appl. Phys. A-Mater.,* 2002, **74**, 355-361

12.   Q. Yang , W. Xu , A. Tomita and T. Kyotani, *Chem. Mater.,* 2005, **17**, 2940-2945

13.   "Carbon Materials for Catalysis", (Serp, Philippe and Figueiredo, Jose Luis), John Wiley & Sons, Inc., Hoboken, New Jersey, 2009.

14.   "ISO 9277:2010. Determination of the specific surface area of solids by gas adsorption - BET method. Second Edition of ISO 9277, ISO", Geneva, 2012.

15.   F. Stoeckli and L. Ballerini, *Fuel,* 1991, **70**, 557-559

16.   P. I. Ravikovitch and A. V. Neimark, *Langmuir*, 2006, **22**, 11171-11179

17.   A. V. Neimark , Y. Lin , P. I. Ravikovitch and M. Thommes, *Carbon*, 2009, **47**, 1617-1628

18.   C. Falco , M. Sevilla , R. J. White , R. Rothe and M. M. Titirici, *ChemSusChem*, 2012, **5**, 1834-1840.

19.   M. Sevilla , A. B. Fuertes and R. Mokaya, *Energy Environ. Sci.,* 2011, **4**, 1400-1410

20.   M. Sevilla , N. Alam and R. Mokaya, *J. Phys. Chem. C*, 2010, **114**, 11314-11319

21.   M. Sevilla , R. Foulston and R. Mokaya, *Energy Environ. Sci.,* 2010, **3**, 223-227

22.   M. Sevilla and A. B. Fuertes, *Energy Environ. Sci.,* 2011, **4**, 1765-1771

23.   M. Sevilla , R. Mokaya and A. B. Fuertes, *Energy Environ. Sci.,* 2011, **4**, 1400-1410

24.   L. Zhao , L. Z. Fan , M. Q. Zhou , H. Guan , S. Qiao , M. Antonietti and M. M. Titirici, *Adv. Mater.,* 2010, **22**, 5202-5206

25.   H. Wang , Q. Gao and J. Hu, *Microp. Mesop. Mat.,* 2010, **131**, 89-96

26.   F. Kapteijn , J. A. Moulijn , S. Matzner and H. P. Boehm, *Carbon*, 1999, **37**, 1143-1150

27.   A. Wahby , J. M. Ramos-Fernández , M. Martínez-Escandell , A. Sepúlveda-Escribano , J. Silvestre-Albero and F. Rodríguez-Reinoso, *ChemSusChem,* 2010, **3**, 974-981

28.   K. T. Chue , J. N. Kim , Y. J. Yoo , S. H. Cho and R. T. Yang, *Ind. Eng. Chem. Res.,* 1995, **34**, 591-598

29.   B. Arstad , H. Fjellvag , K. O. Kongshaug , O. Swang and R. Blom, *Adsorption*, 2008, **14**, 755-762

30.   Y. S. Bae and R. Q. Snurr, *Angew. Chem. Int. Ed.,* 2011, **50**, 11586-11596.

31.	M. R. Mello , D. Phanon , G. Q. Silveira , P. L. Llewellyn and C. M. Ronconi, *Microp. Mesop. Mat.,* 2011, **143**, 174-179.

32.	J. M. Simmons , H. Wu , W. Zhou and T. Yildirim, *Energy Environ. Sci.,* 2011, **4**, 2177-2185.

33.	M. Sevilla and A. B. Fuertes, *J. Colloid Interface Sci.,* -2012, **366**, 147-154

34.	C. Pevida , M. G. Plaza , B. Arias , J. Fermoso , F. Rubiera and J. J. Pis, *Appl. Surf. Sci.*, 2008, **254**, 7165-7172

35.	M. G. Plaza , F. Rubiera , J. J. Pis and C. Pevida, *Appl. Surf. Sci.,* 2010, **256**, 6843-6849

36.	M. Sevilla , P. Valle-Vigón and A. B. Fuertes, *Adv. Funct. Mater.*, 2011, **21**, 2781-2787

37.	C. F. Martín , M. G. Plaza , S. García , J. J. Pis , F. Rubiera and C. Pevida, *Fuel*, 2011, **90**, 2064-2072

38.	L. Liu , Q. F. Deng , T. Y. Ma , X. Z. Lin , X. X. Hou , Y. P. Liu and Z. Y. Yuan, *J. Mater. Chem.*, 2011, **21**, 16001-16009

39.	J. M. Martín-Martínez , R. Torregrosa-Maciá and M. C. Mittelmeijer-Hazeleger, *Fuel*, 1995, **74**, 111-114

40.	A. Vishnyakov , P. I. Ravikovitch and A. V. Neimark, *Langmuir,* 23-9-1999, **15**, 8736-8742

41.	V. Yu. Korovin , V. V. Barkova and V. A. Platonov, *Russian Journal of Applied Chemistry*, 1994, **67**, 237-240

42.	A. A. Énnan , V. S. Kovtun , V. V. Strelko and N. T. Kartel, *Ukrainskii Khimicheskii Zhurnal*, 1987, **53**, 584-586

43.	I. A. Kuzin , A. I. Loskutov , V. F. Palfitov and L. A. Koémets, *Zhurnal Prikladnoi Khimii*, 1972, **45**, 760-765

44.   G. Yushin , R. Dash , J. Jagiello , J. G. Fischer and Y. Gogotsi, *Adv. Funct. Mater.,* 2006, **16**, 2288-2293

45.   W. Shen , S. Zhang , Y. He , J. Li and W. Fan*, J. Mater. Chem.*, 2011, **21**, 14036-14040.

Table 1. Textural properties, and oxygen and nitrogen contents of the porous carbons.

Sample	BET Surface area [$m^2 g^{-1}$]	Pore volume [$cm^3 g^{-1}$]	$V_0 (N_2)$ [$cm^3 g^{-1}$]	$L_0 (N_2)$ [nm]	$V_n (CO_2)$ [$cm^3 g^{-1}$]	O (%)	N (%)
AG-1-700	1480	0.60	0.60	0.92	0.47	11.20	1.76
AG-2-600	1260	0.53	0.51	0.80	0.47	18.22	4.65
AG-2-650	1620	0.68	0.64	0.80	0.50	12.30	2.68
AG-2-700	1940	0.82	0.76	0.92	0.47	11.00	1.47
AG-4-600	1990	0.89	0.76	1.2	0.41	15.26	1.36
AG-4-650	2180	1.01	0.87	1.5	0.36	16.40	1.12
AG-4-700	2390	1.15	0.96	1.8	0.34	9.97	1.09

Table 2. CO_2 capture capacities of the porous carbons at different adsorption temperatures and 1 bar.

Sample	Amount of CO_2 adsorbed, mmol/g (mg/g)			Q_{st} (kJ mol^{-1})[a]
	0 ºC	25 ºC	50 ºC	
AG-1-700	6.7 (292)	4.1 (178)	2.5 (111)	25
AG-2-600	6.2 (273)	4.2 (185)	2.7 (118)	30
AG-2-650	7.0 (306)	4.4 (192)	2.8 (125)	27
AG-2-700	7.4 (325)	4.5 (198)	2.8 (123)	25
AG-4-600	6.2 (274)	3.8 (167)	2.5 (108)	25
AG-4-650	5.9 (260)	3.5 (155)	2.2 (97)	24
AG-4-700	6.1 (267)	3.8 (166)	2.5 (109)	22

[a] Isosteric heat of adsorption determined at a CO_2 surface coverage of 0.7 mmol g^{-1}.

**Table 3.** Highest values of CO_2 capture for porous carbons that can be found in the literature (1 bar).

| Material	Sample code	Amount of CO_2 adsorbed (mmol g^{-1})			Reference
		0ºC	25ºC	50ºC	
N-doped algae-derived AC	AG-2-650	7.0	4.4	2.8	This work
	AG-2-700	7.4	4.5	2.8	
Sawdust-derived AC	AS-2-700	6.6	4.3	2.6	22
	AS-2-600	6.1	4.8	3.6	
TiC-CDC	micro-TiC 600ºC, H$_2$ @ 600ºC	7.1	-	-	1
Petroleum pitch-derived AC	DO-88-M	6.5	4.7	2.9	27
	VR-5-M	8.6	4.2	2.3	
N-doped templated microporous carbons	CEM-750	6.9	4.4	-	2
PAN fiber-derived AC	PAN-PK	-	4.4	-	45
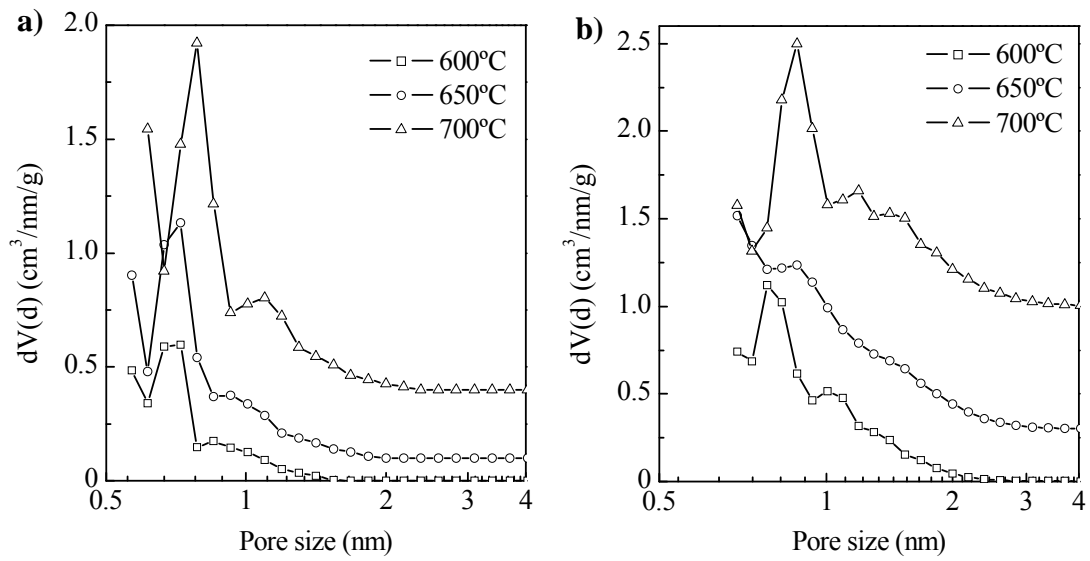
Figure 1. QSDFT pore size distributions of the porous carbons prepared under different activating conditions: a) KOH/HTC carbon = 2 and b) KOH/HTC carbon = 4.
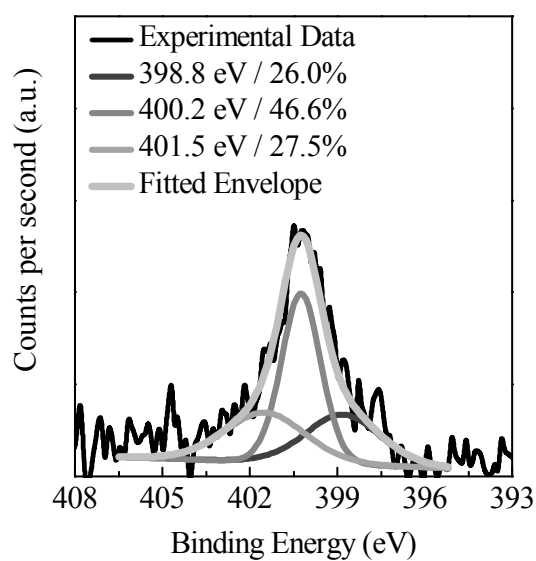
Figure 2. N 1s XPS spectra of AG-2-650.
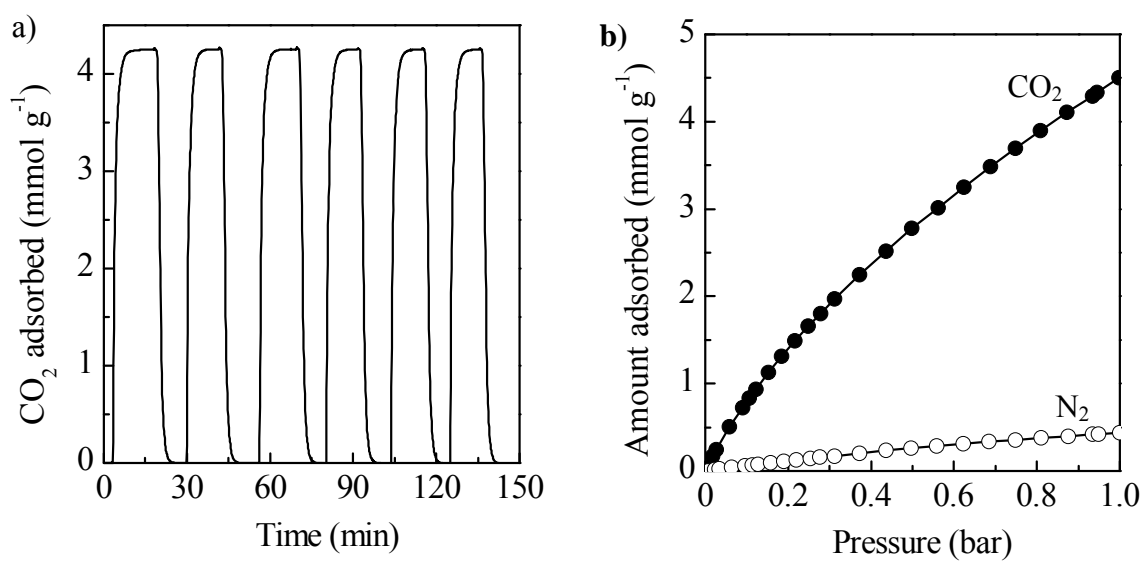
Figure 3. a) CO_2 adsorption-desorption cycles for the sample AG-2-700 at 25 ºC and 1 bar and b) CO_2 and N_2 isotherms at 25 ºC for AG-2-700.
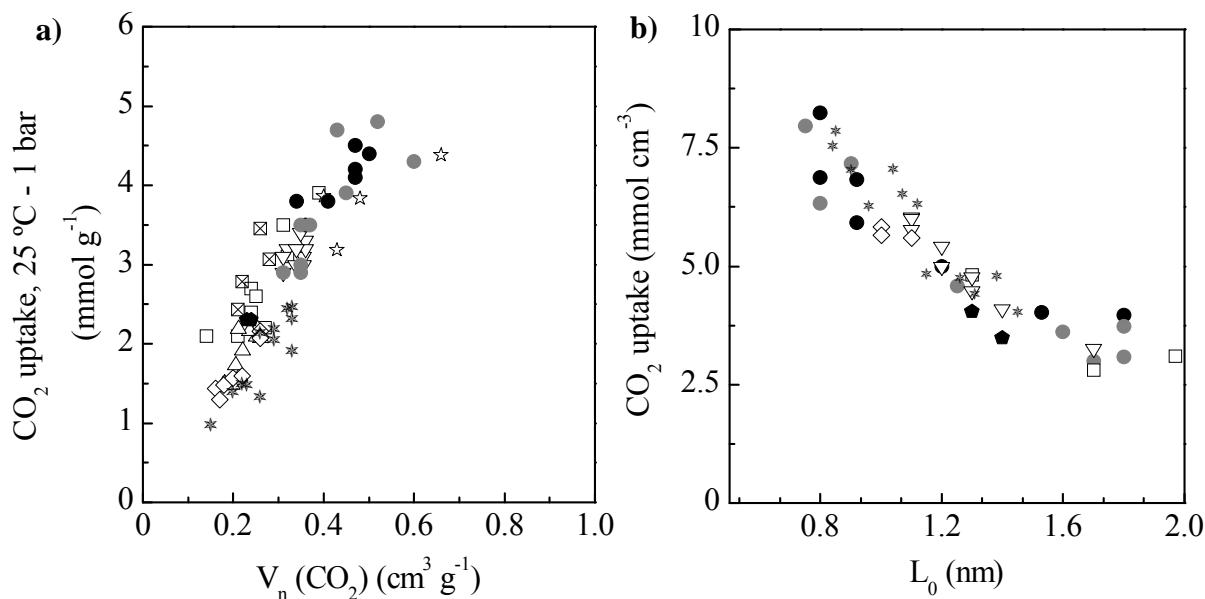
Figure 4. a) Correlation between the CO_2 uptake at 25 °C and 1 bar and the volume of narrow micropores for a variety of porous carbon materials: ● - algae-derived N-doped carbons (this work), ● - HTC-derived carbons (ref. 22), □ - polypyrrole-derived carbons (ref. 36), ▽ - activated templated carbons (ref. 33), ☆ - N-doped zeolite templated carbons (ref. 2), △ - N-doped activated carbons (ref. 34), ◇ - ammoxidised carbons (ref. 35), ✳ - phenol-formaldehyde resin-derived activated carbons (ref. 37) ⊠ - N-doped ordered mesoporous carbons (ref. 38) and ⬠ - two commercial activated carbons measured in our lab (Super and Supra DLC-50 by Norit). b) Average pore width and CO_2 uptake (at 0 °C and 1 bar) per total volume of micropores of the porous carbon materials.